Jurnal Teknologi

Full paper

Electrical Capacitance Tomography (ECT): An Improved Sensitivity Distribution Using Two-Differential Excitation Technique

Elmy Johana Mohamad[a*], Hanis Liyana Mohmad Ameran[a], Ruzairi Abdul Rahim[b], Omar Md. Faizan Marwah[c]

[a]*Jabatan Kejuruteraan Mekatronik & Robotik, Fakulti Kejuruteraan Elektrik & Elektronik, Universiti Tun Hussein Onn Malaysia, Malaysia*
[b]*Process Tomography and Instrumentation Engineering Research Group (PROTOM-i), Infocomm Research Alliance, Faculty of Electrical Engineering, Universiti Teknologi Malaysia, 81310 UTM Johor Bahru, Malaysia*
[c]*Jabatan Kejuruteraan Mekanikal & Pembuatan, Fakulti Kejuruteraan Pembuatan & Industri, Universiti Tun Hussein Onn Malaysia, Malaysia*

[*]Corresponding author: elmy@uthm.edu.my

Article history

Received :9 November 2014
Received in revised form :
15 January 2015
Accepted :15 March 2015

Graphical abstract

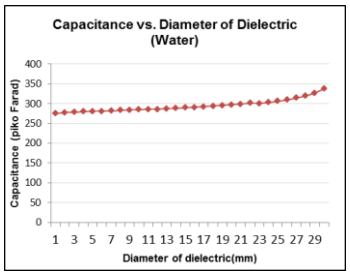

Linear relationship between capacitance and diameter of electric with permittivity ε_r=80, using two-differential excitation potentials/voltage source

Abstract

In this study, we propose the use of the two-differential potential excitation technique in an Electrical Capacitance Tomography (ECT) system to improve: (1) the non-uniform sensitivity distribution caused by the non-uniform potential distribution in the central area; and (2) the nonlinear relation between capacitance and material permittivity. A simulation of a 16-segmented ECT system is developed using COMSOL Multiphysics to observe the changes of the inter-electrodes capacitances and the permittivity of the dielectric material when two differential excitation potentials are injected. Generated phantoms and measured values are presented. An experiment using the real system is also carried out to verify the simulations results. By using this technique, it was shown that the relationship between the capacitances measured from inter-electrodes and the permittivity became more linear. In addition, potential distribution is increased in the central area indicating an increase in the sensitivity distribution in the central area. The use of this technique increases the level of detected signals and improves the SNR (signal-to-noise ratio) as compared to those achieved using standard single-voltage source methods.

Keywords: ECT; permittivity distribution; differential excitation potentials; COMSOL Multiphysics

Abstrak

Di dalam kajian ini, kami memperkenalkan satu teknik baru di dalam sistem Tomografi Kapasitan Elektrik (TKE) iaitu penggunaan dua potensi elektrik sebagai sumber eksitasi elektrod, dengan tujuan untuk memperbaiki: (1) distribusi potensi di bahagian tengah paip, dan (2) hubungan tidak linear antara bacaan kapasitan dan ketelusan bahan dielektrik. Simulasi sistem TKE dengan 16 segmen telah dijalankan menggunakan COMSOL Multiphysics untuk memerhati perubahan kapasitan di antara elektrod dan ketelusan bahan dielektrik apabila teknik baru ini digunakan. Eksperimen menggunakan sistem TKE sebenar juga dijalankan supaya hasil simulasi dapat disahkan. Teknik baru yang diperkenalkan terbukti berjaya menjadikan hubungan kapasitan dan ketelusan bahan lebih linear. Kesensitifan sensor juga dapat ditingkatkan di bahagian tengah paip, sekaligus menaikkan datar signal yang diterima berbanding dengan penggunaan teknik satu potensi voltan.

Kata kunci: Tomografi Kapasitan Elektrik; distribusi ketelusan; dua potensi eksitasi; COMSOL Multiphysics

1.0 INTRODUCTION

Since the introduction of tomography in the 1950's, its applications have essentially evolved from medical to industrial use (called process tomography) in the 1970's. Nowadays, process tomography systems play an essential role in the industrial environment as they provide means to monitor process flows without altering or stalling the industrial processes. Along with providing the cross-sectional images of closed pipes or vessels, these systems offer important flow information such as concentration profile, velocity profile, flow rate and compositions.

Electrical Capacitance Tomography (ECT) is one of tomography techniques based on measuring the electrical properties of the material(s) inside a closed space. It examines the internal permittivity distribution of the investigated material using external capacitances. ECT is an attractive and promising method

for the measurement of two-phase flow as this measurement technique is able to differentiate materials based on their permittivity. Besides, ECT offers non-invasive measurement with high-speed capabilities and good reliability. ECT has been utilized successfully in numerous industrial applications of multiphase flow[1-4].

However, there are known principal difficulties of image reconstruction using the conventional ECT system: (1) the nonlinear relationship between the permittivity distribution and capacitance due to the distortion of electric field caused by the existence of the material in the vicinity (also known as fringe capacitance effect)[1,3,5]; and (2) the poor signal-to-noise ratio (SNR) in the central area of pipes as the sensor is more sensitive near the pipe wall than in the central area (a typical maximum sensitivity of an adjacent electrode pair in an 12-electrode ECT sensor with single-electrode excitation and single-electrode detection is 100 times larger than that of an opposing electrode pair[1]), and consequently causes the mutual capacitances to be small, which leads to small electrode charges (and their change)[1,6].

An ECT is a soft-field sensing method which means the sensor field is sensitive to the component parameters distribution, both inside and outside the measurement volume. The stray electric fields from the sensors will cause fringe capacitance effect thus alter the measured standing capacitance between electrodes. For sensors with internal electrodes, the capacitance caused by the electric field inside the sensor will always increase in proportion to the material permittivity when the sensor is filled uniformly with a higher permittivity material. The wall has a negative effect on the measurement of the internal capacitance because the wall capacitance is effectively in series with the internal capacitance[5]. However, in the case of external electrodes sensor, which is used in this project, the permittivity of the wall causes nonlinear changes in capacitance. The capacitance value may increase or decrease depending on the wall thickness, permittivity of the sensor's wall and permittivity of its contents[7]. In addition, the nonlinear change of the capacitance due to an increase in conductivity has been reported through software simulation and experiment[8]. As the conductivity increased, the inter-electrode capacitance increased and became less sensitive to the permittivity distribution in the sensing region.

The conventional method of measuring the capacitances between all electrode pairs in ECT system is the single-electrode excitation scheme, where only one excitation potential or source is applied to each of the sensor's electrodes in turn (while the remaining electrodes kept at ground potential). It has been stated that the sensitivity is proportional to the electrical field strength[9].

There are only few techniques proposed in earlier studies that focus in improving the sensitivity, thus the SNR in the central area. For example, a scheme called parallel field excitation has been proposed previously[5,10]. In this scheme, the parallel field is generated by applying excitation signals to all electrodes. However, if excitation signals are applied to multiple electrodes, it is possible to generate a parallel field within the ECT sensor. The sensitivity maps of a parallel-field ECT sensor are simply linear superimpositions of the sensitivity maps of the conventional ECT sensor, and therefore, a parallel-field ECT sensor still does not have a uniform sensitivity distribution.

In this work, we propose the use of two-differential potentials excitation sources scheme instead of the single excitation source scheme which is conventionally used. Two-differential potential excitations are injected to electrode pairs to create a considerably uniform excitation field across the sensor. This technique has never been applied in an ECT system before. The SNR (signal noise to ratio) can be improved proportionally with the increase in voltage across the center of the pipes.

2.1 Single Excitation Potential

The standard excitation scheme used in an ECT system consists of the injection of a single potential power source into the electrode. Each of sixteen electrodes is excited at a time with similar excitation source. All other electrodes will act as the detectors and remain at zero potential. The capacitances between the excited electrode and each of its detecting electrode pairs are measured. For example, when the first electrode is excited and all other electrodes are at zero potential, the charges between electrode 1 and electrodes 2–16 are measured and noted $C_{2\text{-}1}$–$C_{16\text{-}1}$. This procedure was repeated by applying voltage to electrode n and measuring the charge on the electrodes up to 16, until, as a final step, voltage is applied to electrode 15 and the charge of 16 electrodes is measured. In this way, 120 independent mutual capacitance values were produced. In this project, a 25 V_{pp} signal is used as the excitation source.

2.2 Two-Differential Excitation Potentials

We introduce a new scheme called two-differential excitation potentials technique. A two-differential voltage source is applied at an electrode pair. In the first step, to obtain a complete set of data for one image, the first electrode (electrode 1) becomes the excitation electrode/source electrode (which is supplied with a sine wave), while all the other electrodes act as receivers, and receive the capacitor value corresponding to the dielectric in between. For example, capacitances between electrodes 1 and 2, 1 and 3, 1 and 4 until the adjunction electrode, electrode 1 and 14, 1 and 15 and the last electrode 1 and 16 are measured, in parallel. In this time, when electrode 1 was injected by the source, electrodes other than electrode 1 are at the virtual earth potential imposed by the transducer and they are called the detecting electrode.

During this measurement phase, electrode 1 was injected by two differential excitation potentials/voltage sources ($4V_{pp}$ and 24 V_{pp}) sequentially, where the lower excitation voltage source $4V_{pp}$ will excited to receive adjunction electrode pairs, for example; 1 and 2, 1 and 3, 1 and 4 also 1 and 14, 1 and 15 then 1 and 16, while an opposing electrode pair, in this case electrode 5 until electrode 13, will receive a high voltage excitation source of 24 V_{pp}. In the next step, electrode 2 acts as excitation and electrodes 3-16 are used for detection, obtaining 14 capacitance measurements. This process continues until electrode 15 is used for excitation and electrode 16 for detection, which obtains only one capacitance measurement. In this case, there will be 120 independent capacitance measurements. In general, the number of independent capacitance measurements is governed by $N(N-1)/2$, where N is the number of electrodes.

3.0 METHODOLOGY

In order to analyse the capability of the proposed technique, both simulative and experimental study of a 16-segmented ECT system were done. We verify the performance of this technique by comparing the simulation and experiment results when two-differential potential excitation is injected to the sensor with the results obtained using the standard single potential excitation source. The simulation of ECT sensor allows us to analyse the permittivity distribution by observing the deflection of electric field lines inside the pipe when the electrodes are excited. In this work, we also investigate the changes of capacitance when the diameter of the dielectric with the higher permittivity increases. Annular phantoms with different combinations of dielectric permittivity are generated for the simulations and experiments.

3.1 ECT Simulation

The simulative study could be done by using commercial multi-purpose simulation software e.g. COMSOL Multiphysics and MATLAB, or by custom designed solvers[11, 12]. In this work, we create a forward modeling of the real ECT sensor using COMSOL Multiphysics. The software is able to quantify the capacitance measurements between electrodes when an electric field is applied; and to obtain the permittivity distribution inside the closed pipe from the sensor by applying the Linear Finite Element Method (FEM). The capacitance sensor model design in COMSOL holds the purpose to apply numerical calculation for defining the electric potential within the sensor. This indicates that it can solve the problem of ECT forward which is to calculate the capacitances between all possible electrode pairs.

The shape of a pipeline is drawn as the first step in developing the numerical modeling. The shape of a pipeline is actually an illustration of a circle with some particular diameter. As for this case, the applied drawing geometry will have to follow the actual size and geometry of the hardware. Figure 1 illustrates the 16-electrodes sensor arrangement which was used in this work. Each electrode plate is 120 mm in length. The sensor has been designed to cover an acrylic pipe with a diameter of 110 mm and a wall thickness of 0.5 cm.

In this simulation, the geometry comprises the spatial discretisation of the sensor inner part. This technique is called FEM meshing and its purpose is to acquire a consistent definition in the area to be observed. This is also to get a higher definition near the electrodes, where more accuracy electrode-pairs are required by means of the method described in.

To obtain the potential distribution and the electrical field lines within the space of the sensor, we analyse the potential difference between the excited electrodes and the detecting electrode. This will allow the verification of the potential difference between inter-electrode capacitance.

We firstly observe the permittivity distribution inside the pipe when we fill it with single type of dielectric which is water. We then generate different types of annular phantoms where we fill them with different permittivity values to further investigate the changes of capacitance due to the materials permittivity. We injected both type of excitation for each simulation and compare the results.

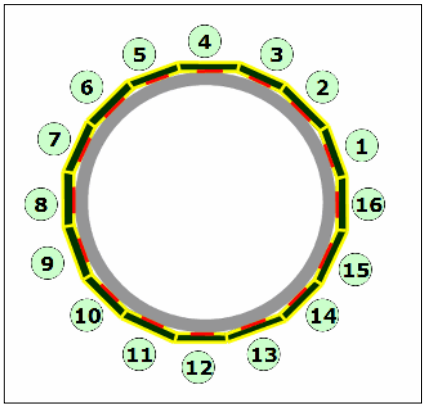

Figure 1 16-segmented sensor arrangement

3.2 ECT Hardware Development & Experimental Setup

An ECT sensor is developed in this work and will be used to analyse the performance of the proposed technique. Experiments were performed to compare the distribution of potentials between using two differential excitation potentials and using the conventional technique, which only applies one excitation potential. The charges of the opposing electrodes to the adjunction electrode, which was the last electrode, were measured.

The new approach of the developed sensing module is the integration of intelligent electrode sensing circuit on each of electrode sensors. A microcontroller unit and data acquisition (DAQ) system has been integrated on the electrode sensing circuit, making the sensor able to work independently. Each of the circuits consists of; signal switching circuit, signal detection and amplifier circuit, absolute value circuit, low pass filter circuit, programmable gain amplifier (PGA), analog to digital converter circuit and a microcontroller control unit. The desired sequence operation of electrode's signal selection, measuring data and conversion data depends on the microcontroller programming.

The electrode sensors in this research is designed in a way that it can be plugged directly onto the printed circuit board (PCB) sockets of the signal conditioning circuit and becomes a single sensing module. Figure 2 shows the block diagram of a sensing module. Each of the electrodes is connected to a signal conditioning circuit via 1.0 mm pitch PCB connectors as shown in Figure 3.

Other than that, the driven guard that usually placed between adjacent measuring electrodes and earth screen has been embedded on the segmented electrode sensor plates. This eliminates the cable noise and the electrode, so the signal conditioning board can be expanded according to pipe diameter.

These sixteen boards are interconnected by using a 26 way IDC cable. This design has eliminated the need to use cables to connect the electrodes and signal conditioning circuits. In the case where only one sensing module is malfunctioning, users can simply change it by unplugging the board and replacing it with a new board. The actual module is shown in Figure 4.

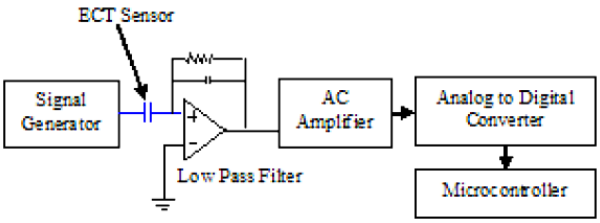

Figure 2 Block diagram of the sensing module

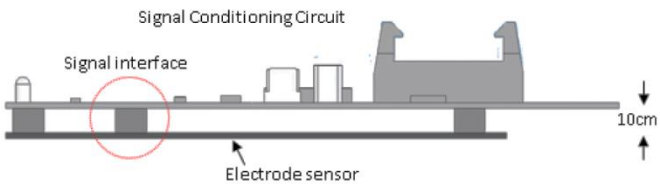

Figure 3 Illustration of the sensing module

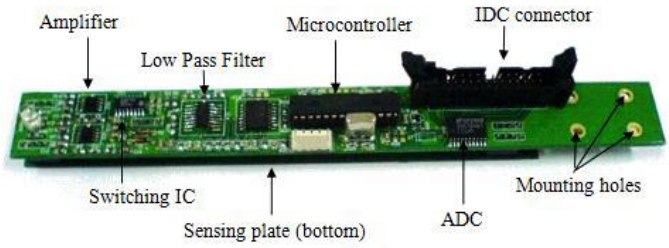

Figure 4 Photo of the actual sensing module

The changes of capacitance due to the different materials permittivity are observed using the developed sensing module. Annular phantoms of water/air flow were created using bottles and test tubes of different diameters, as shown in Figure 5. The annular water/air flow phantom was created by inserting the bottle and test tube into the ECT sensor, then filling up the bottle and test tube with water, and leaving a space between the inner ECT sensor wall and the outer bottle or test tube wall as representation of air. Tap water with a relative permittivity, ε_r of 80 was used in the experiments. The diameter of water tubes is increased throughout the experiment and we measure the corresponding inter-electrode capacitances when single excitation source is injected (Figure 6) to the sensor. We repeat the experiment using two-differential excitation potential source (Figure 7).

Figure 5 Portable segmented ECT with bottle and test tube used to create phantoms inside the ECT sensor. The bottle and test tube were filled with water, creating a phantom of annular water flow

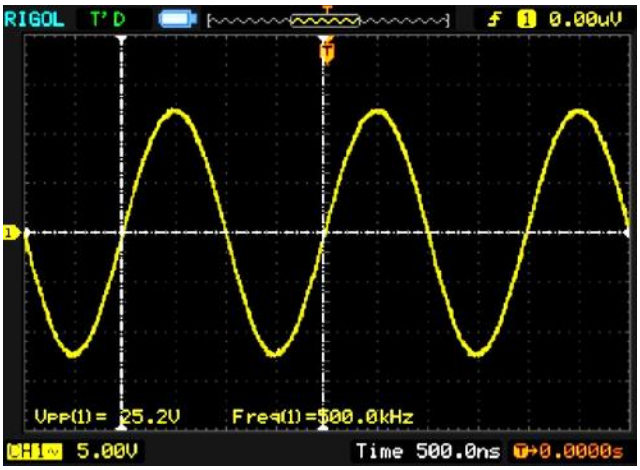

Figure 6 Transmitted signal from the signal generator with single excitation potentials/voltage source

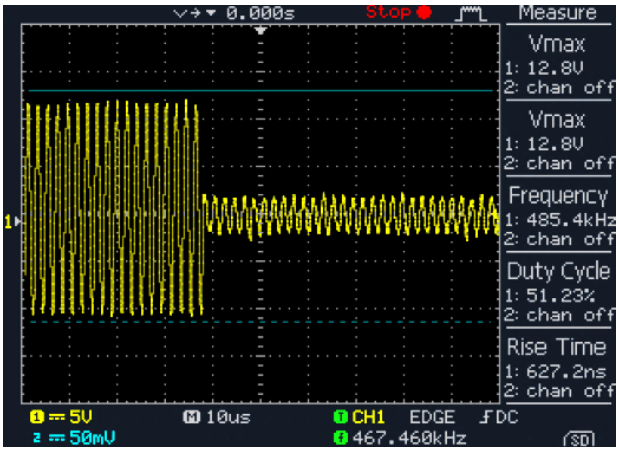

Figure 7 Sequentially transmitted signal from the signal generator with two difference potentials/voltage source

4.0 RESULTS & ANALYSIS

In this chapter, we present the results of the simulations and experiments done. There are two necessary main observation points in analysing the performance of the proposed technique as compared to the conventional technique which are:

4.1 Permittivity Distribution

Figure 8 presents a schematic illustration of: (a) potential distribution inside the sensor space and (b) electric field lines that present between any of the two electrodes when electrode 4 is excited while the pipe is filled with water. Figure 9 shows the electric field lines inside the same pipe when each electrode is excited in turn while the others are kept at zero potential. The potential concentration across the pipe is also described in Figure 9 and indicated by the rainbow color scale where: blue being the area with the highest potential concentration; and red is the lowest.

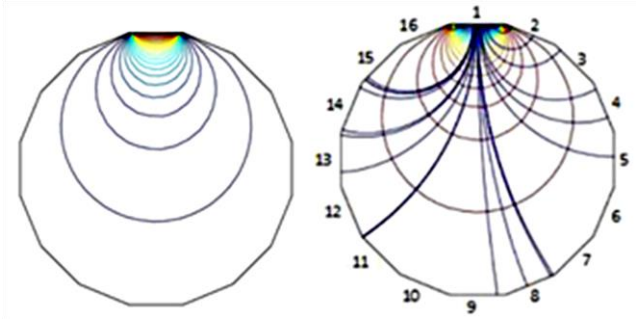

Figure 8 (a) Potential Distribution and (b) Electrical field when single electrode is excited (electrode 1).

We can see that the opposing electrodes' potential distribution line in the sensing area is not widely covered. Like mentioned earlier, the adjacent electrode pair's sensitivity is typically 100 times larger compared to the opposing electrode pair in a 12-electrode ECT sensor with single excitation and single detection electrode[1], resulting in the higher sensitivity near sensors' wall rather than the pipe's central area. Therefore, this has become the reason of poor SNR in the central area and the relatively small mutual capacitances value. The electrode charges (and their change) will consequently become small, thus resulting in a poor SNR measurement.

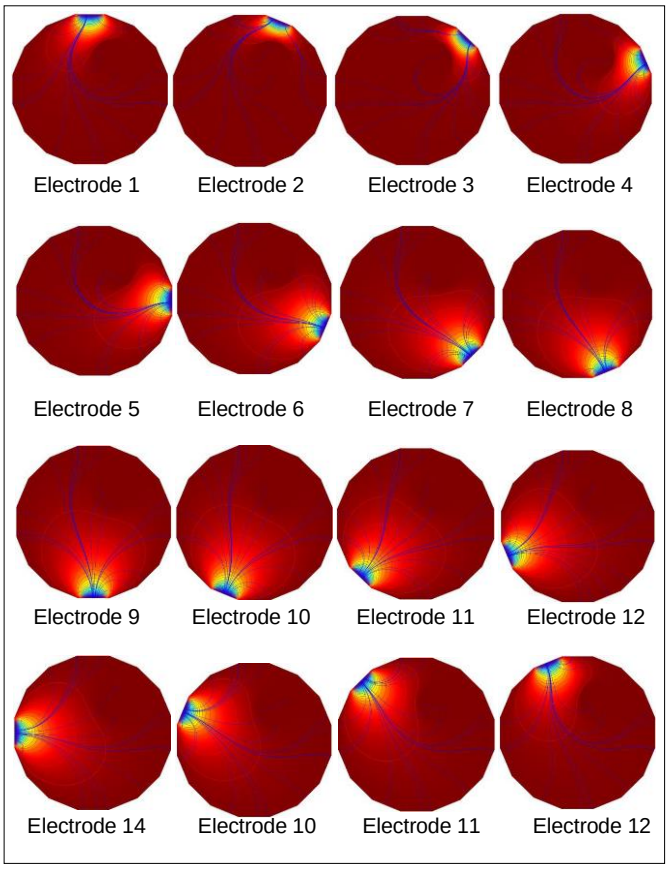

Figure 9 Electric field lines are deflected depending on material distribution, when each electrode was excited

We further investigate the permittivity distribution inside the pipe by using a 50 mm diameter cylindrical phantom of water enclosed by air where its center is located at coordinates x = 70 mm and y = 130 mm. The capacitance was measured between the electric field distribution and the model electrode pairs for two-dimensional (2D) (Figure 10 (a)) and three-dimensional (3D) (Figure 10(b)) simulations, when electrode 1 was excited. The figures obtained from these simulation shows that the electric field lines are deflected, and its angle of deflection relies on the material distribution.

In order to understand more about the relation between deflection of electric field and the permittivity distribution, we used six different phantoms with different combinations of materials with different permittivity (air, water, oil) as described in Figure 11.

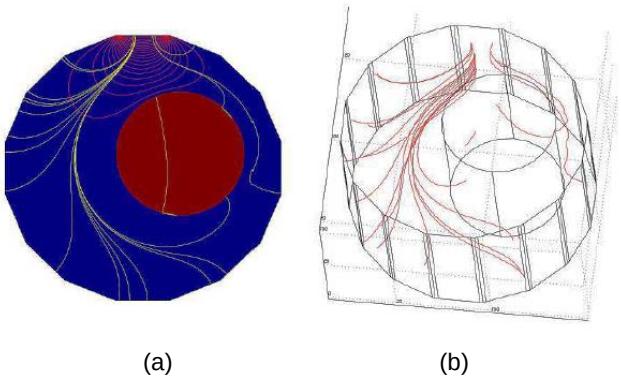

Figure 10 Permittivity distributions for different types of dielectric. Results from (a) 2D and (b) 3D simulation. The blue area is the sensing region representing air (ε_{air} =1), and red area represents water (ε_{water} =80)

We observe in Figure 11 (a) – (f) that the degree of penetration of the electrical field is subject to the material permittivity. Theoretically, water has the highest permittivity (ε_{water} is 80) between oil (ε_{oil} is 3.25) and air, which has the lowest one (ε_{air} is 1). The electrical fields seem to be deflected more when the permittivity is higher (the water compared to the oil or air). This corresponds to the simulation results, where the degree of reflected electrical field seems to increase when the permittivity increases. Furthermore, when the phantom permittivity becomes higher due to an increase in conductivity, the electrical field lines also seems to bend more around the phantom.

Figure 12 shows the simulation by two differential excitation potentials which started with electrode 1 becoming the excitation electrode, followed by electrodes 2, 3, 4, 5, 6 etc. The electrical potential distribution inside the pipe is represented using the rainbow color scale where the lowest potential is in blue and red represents the highest potential.

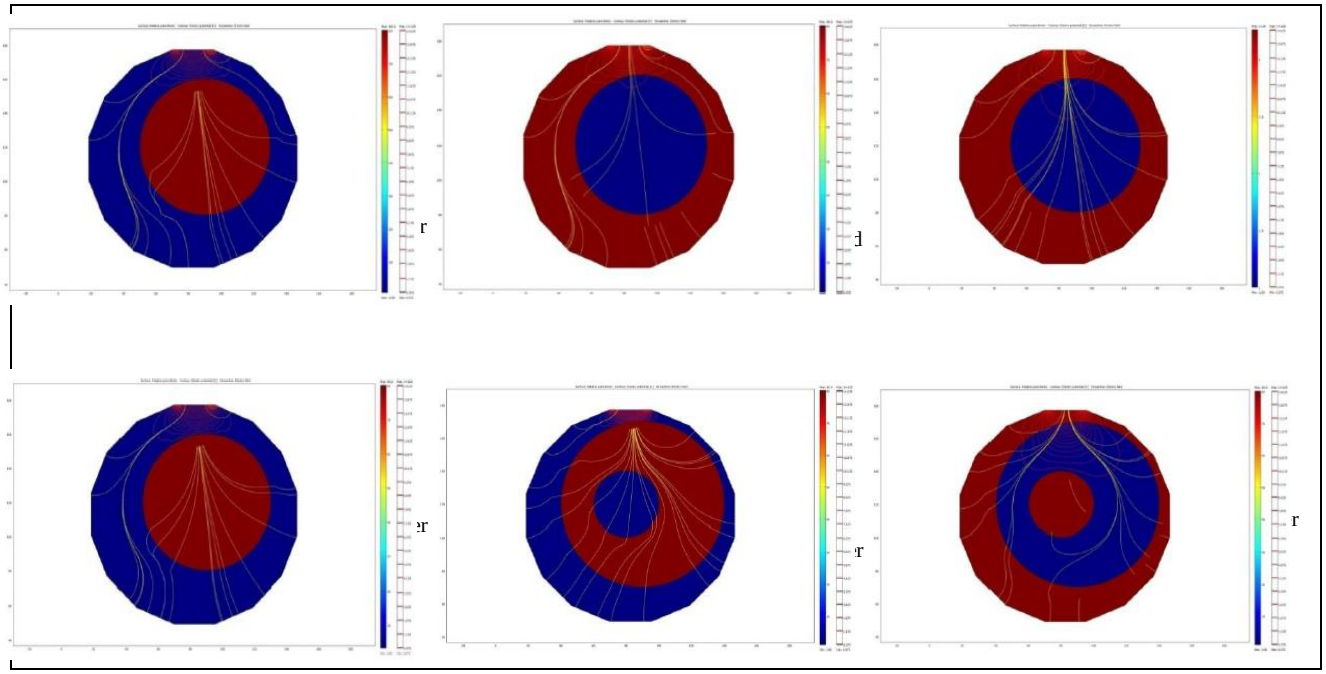

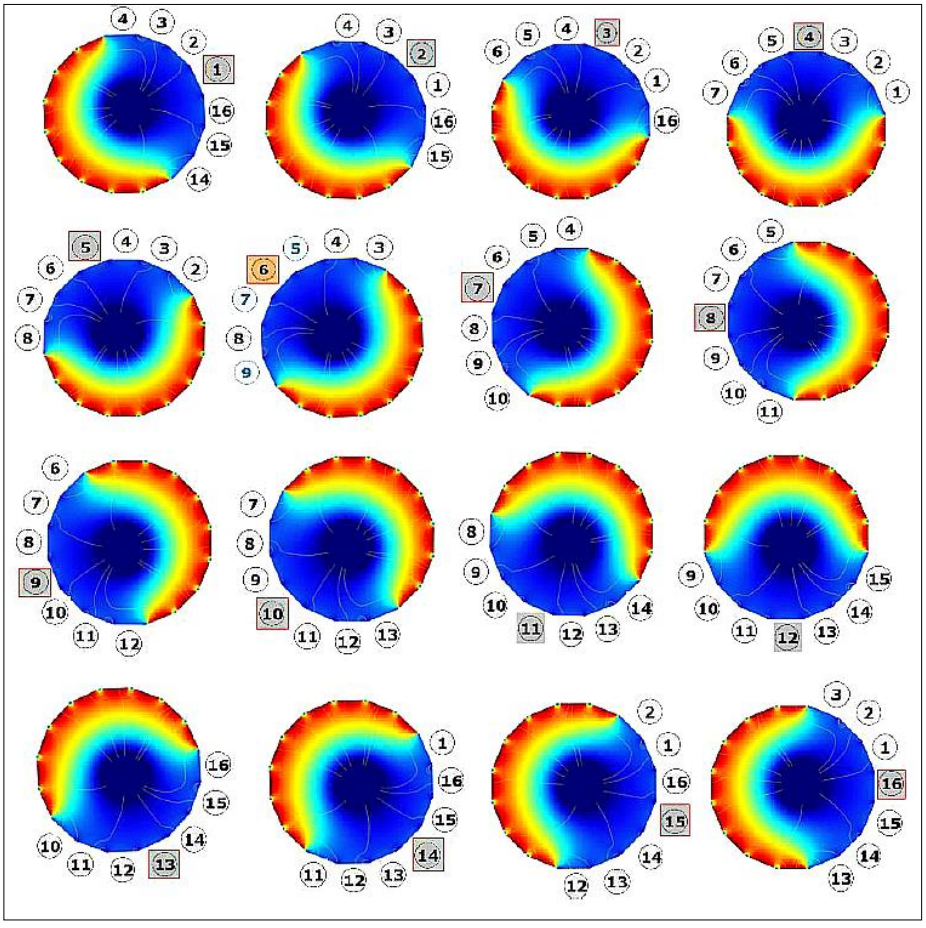

Figure 12 Electrical field distributions for 2D when half of electrode pairs were excited with low voltage source and another half with higher voltage source

4.2 Analysis of Diameter Increase of the Higher Dielectric Material

In this research, we analyze the non-linear changes of capacitances when the diameter of the higher dielectric material is increased. By using the COMSOL Multiphysics simulation, the capacitance is implemented between the model electrode-pairs. The effect of the permittivity size increase to both excitation scheme is analyzed as due respect to the annular phantom. Figure 13 illustrates the results of the higher dielectric material diameter increase where blue (air) and red (water) for both excitation scheme. The image indicates that the electric field lines incline to follow more of the phantom shape alongside the increasing of dielectric diameter when using two different potentials excitation as compared to when using single excitation scheme.

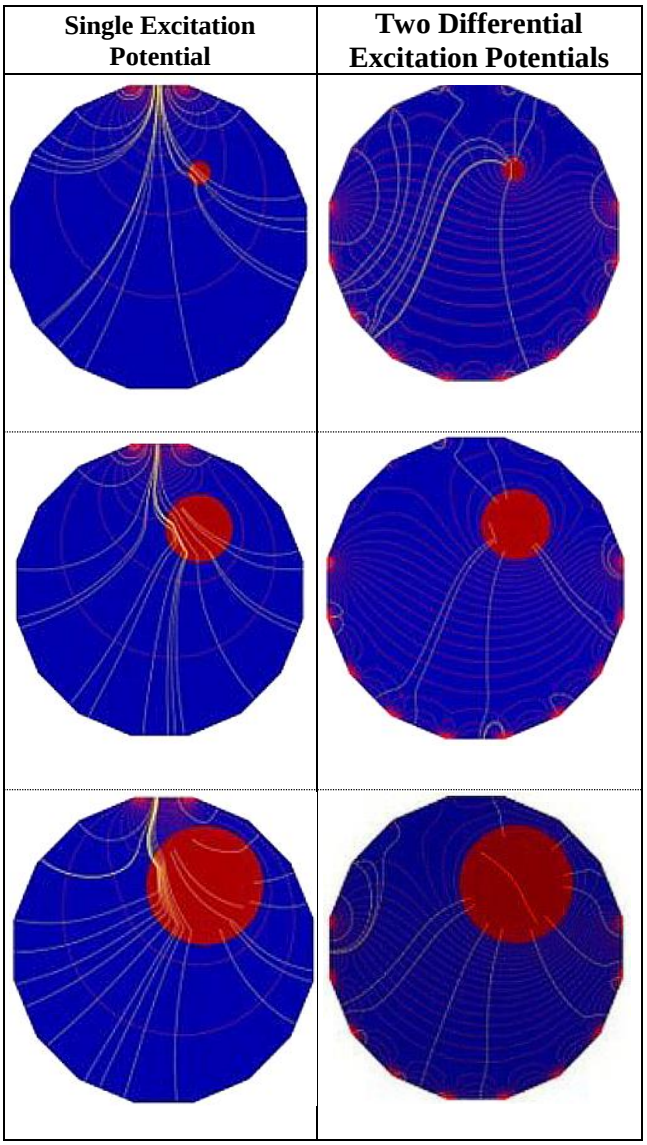

Figure 13 Reconstructed simulation images when increasing the size of permittivity material using single and two differential potentials/voltages source

Figure 14 shows the potential distribution measured with water filled phantom. The standing capacitances of the nearest two conducting materials produce a higher density of magnetic field, and therefore generate a higher standing. Figure 15 shows the capacitance changes between opposing electrodes as well as the dielectric material permittivity with single excitation schemes. The standing capacitance show non-linear regression changes as a result of the permittivity material size increase are presented in the data collected

The capacitance components reacting to the electrical field within the sensors will increase in proportion at all time to the material permittivity for a sensor with internal electrodes. This is provided if the sensor is filled with uniformly higher permittivity material. On the other hand, the wall permittivity will initiate non-linear changes in capacitance for the sensor with external electrodes. This might increase or decrease which is determined by the thickness of the wall as well as the permittivity of the sensor wall and contents.

The capacitance changes between opposing electrodes and the dielectric material permittivity with the use of two different excitation potentials schemes are depicted in Figure 16. A linear regression is sensible for the majority of the reading for Figure 15. However, whenever the phantom diameter increases, the capacitance will rapidly increase.

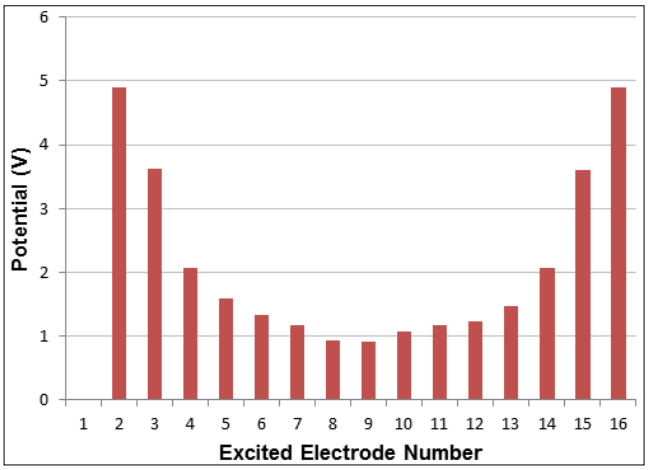

Figure 14 Potential distribution for the permittivity of the dielectric material, εr=80, using single potential/voltage source scheme

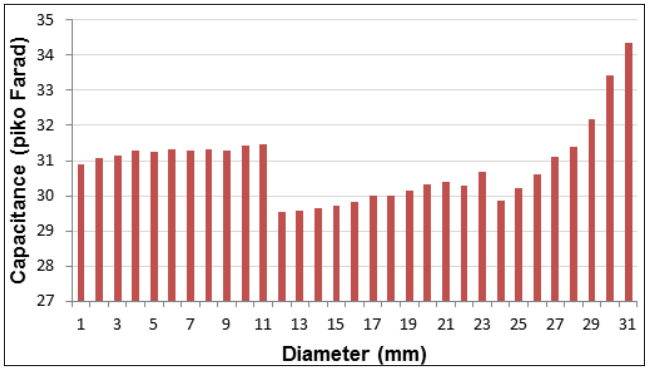

Figure 15 Simulated capacitances due to increasing the size of permittivity of the dielectric material, εr=80, using singlel potential/voltage source scheme

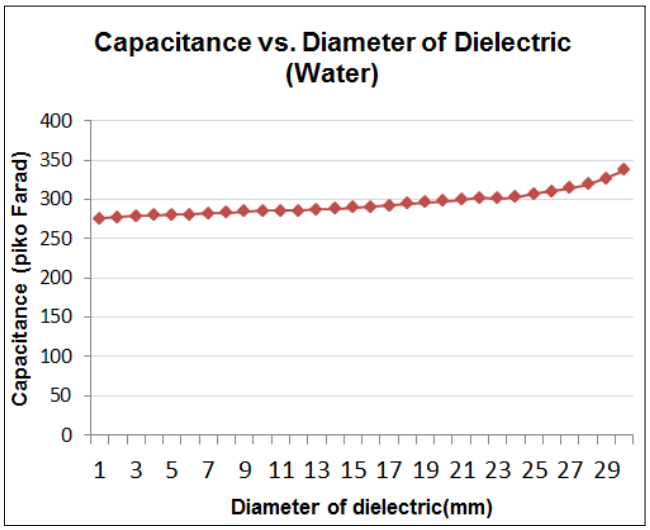

Figure 16 Simulated capacitances due to increasing of the permittivity size of the dielectric material, ε_r=80, using two different potentials/voltage source schemes

Acknowledgement

Authors are grateful to the financial support by Research University Grant of Universiti Teknologi Malaysia (Grant No. Q.J130000.7123.00J04) and ScienceFund of Ministry of Science, Technology & Innovation, Malaysia (Grant No. 03-01-06-SF0193; Vot 79128).

References

[1] Yang, W. 2010. Design of Electrical Capacitance Tomography Sensors. *Measurement Science and Technology*. 21(4): 233–957. DOI: 10.1088/0957-0233/21/4/042001.

[2] Chaplin, G., T. Pugsley, L. Van Der Lee, A. Kantzas and C. Winters. 2005. The Dynamic Calibration of An Electrical Capacitance Tomography Sensor Applied to the Fluidized Bed Drying of Pharmaceutical Granule. *Measurement Science and Technology*. 16(6): 1281–1290. DOI: 10.1088/0957-0233/16/6/007.

[3] Yang, W., and L. Peng. 2003. Image Reconstruction Algorithms for Electrical Capacitance Tomography. *Measurement Science and Technology*. 14(1):1–3. DOI: 10.1088/0957-0233/14/1/201.

[4] Yang, W. 2007. Tomographic Imaging based on Capacitance Measurement and Industrial Applications. *IEEE International Workshop on Imaging, Systems and Techniques-IST 200 Proceedings 7*. May 4–5. DOI: 10.1109/IST.2007.379587.

[5] Daoye, Y., Z. Bin, X. Chuanlong, T. Guanghua and W. Shimin. 2009. Effect of Pipeline Thickness on Electrical Capacitance Tomography. *Journal of Physics: Conference Series*. 147(1): 012030. DOI: 10.1088/1742-6596/147/1/012030.

[6] Gamio, J. 2002. A Comparative Analysis of Single and Multiple-Electrode Excitation Methods in Electrical Capacitance Tomography. *Measurement Science and Technology*/. 13(12): 1799–1809. DOI: 10.1088/0957-0233/13/12/301.

[7] Yang, W., C. Xie, J. Gamio and M. Beck. 1995. Design of a Capacitance Tomographic Imaging Sensor with Uniform Electric Field. *Process Tomography: Implementation for Industrial Processes*. 266–276.

[8] Alme, K. and S. Mylvaganam. 2006. Analyzing 3D and Conductivity Effects in Electrical Tomography System Using COMSOL Multiphysics EM Module. Nordic COMSOL Conference Proceedings.

[9] Yang, W., D. Spink, J. Gamio, and M. Beck. 1997. Sensitivity Distributions of Capacitance Tomography Sensors with Parallel Field Excitation. *Measurement Science and Technology*. 8: 562–569. DOI: 10.1088/0957-0233/8/5/016.

[10] Yu, Z., G. Lyon, S. Zeiabak, H. Tan, A. Peyton and M. Beck. 1995. Towards Optimising the Sensitivity Distribution of Electrical Tomography Sensors. 7th Conference on Sensors and their Applications Proceedings. 10–13 September: 278–83. ISBN: 075030331X.

[11] Kryszyn, J., W.T. Smolik, R. Szabatin and J. Mirkowski. 2012. Electric Field Simulation in Electrical Capacitance Tomography. 2012 *IEEE International Conference on Imaging Systems and Techniques (IST) Proceedings*. 595–598. DOI: 10.1109/IST.2012.6295592

[12] Schlegl, T., T. Bretterklieber, S. Muhlbacher-Karrer and H. Zangl. 2014. Simulation of the Leakage Effect in Capacitive Sensing. International *Journal on Smart Sensing & Intelligent Systems*. 7(4). ISSN: 1778-5608.

[13] Chan, K. 2008. Electrical Capacitance Tomography (ECT) System with Mobile Sensor for the Liquid Measurement. *Unpublished Thesis of Master Degree in Electrical Engineering*. Universiti Teknologi, Malaysia.

[14] Elmy, J. and R. Abdul Rahim. 2010. Multiphase Flow Reconstruction in Oil Pipelines by Portable Capacitance Tomography. *IEEE Sensors Conference 2010 Proceedings*. 273–278. DOI: 10.1109/ICSENS.2010.5689865.

[15] Soleimani, M., C. Mitchell, R. Banasiak, R. Wajman and A. Adler. 2009. Four Dimensional Electrical Capacitance Tomography Using Experimental Data. *Progress in Electromagnetics Research, PIER*. 90: 171–186. DOI: 10.2528/PIER09010202.

[16] Marashdeh, W., L. Fan and F. Teixeira. 2006. A Nonlinear Image Reconstruction Technique for ECT Using a Combined Neural Network Approach. Measurement Science and Technology. 17: 2097–2103. DOI: 10.1088/0957-0233/17/8/007.

[17] Banasiak, R., R. Wajman, D. Sankowski, and M. Soleimani. 2010. Three-Dimensional Nonlinear Inversion of Electrical Capacitance Tomography Data Using a Complete Sensor Model. *Progress in Electromagnetics Research, PIER*. 100: 219–234.